Journal of Power Sources 221 (2013) 49–56

Contents lists available at SciVerse ScienceDirect

Journal of Power Sources

journal homepage: www.elsevier.com/locate/jpowsour

Electrodeposition of polypyrrole–carbon nanotube composites for electrochemical supercapacitors

X. Li, I. Zhitomirsky*

Department of Materials Science and Engineering, McMaster University, 1280 Main St. West, Hamilton, Ontario, Canada L8S 4L7

HIGHLIGHTS

- ► Composite polypyrrole–carbon nanotube films were obtained electrochemically.
- ► Pyrocatechol violet was used as anionic dopant, dispersing and charging agent.
- ► Composite films were investigated for applications in electrochemical supercapacitors.
- ► Stainless steel foils and porous nickel plaques were used as current collectors.
- ► Nickel plaques allowed higher capacitance and higher materials loading.

ARTICLE INFO

Article history:
Received 3 June 2012
Received in revised form
3 August 2012
Accepted 6 August 2012
Available online 11 August 2012

Keywords:
Electropolymerization
Polypyrrole
Carbon nanotube
Composite
Film
Capacitance

ABSTRACT

In this work we introduce a new electrochemical strategy for the fabrication of composite polypyrrole (PPY)–multiwalled carbon nanotube (MWCNT) composites for electrochemical supercapacitors (ES). The problem of low adhesion of PPY films on stainless steel and Ni substrates is addressed by the use of pyrocatechol violet (PV) dye as an anionic dopant. The experimental data indicates that strong adhesion of PPY films is attributed to catecholate type of PV bonding. We also find that PV strongly adsorbs on MWCNT and allows efficient dispersion, charging and controlled electrophoretic deposition (EPD) of MWCNT. The use of PV for electropolymerization of PPY and EPD of MWCNT allows the formation of composite films by combined electrodeposition method. Results show that Ni-plaque current collectors developed for high power battery applications can be electrochemically impregnated with PPY–MWCNT to form electrodes for ES. Ni plaque based electrodes offer advantages of significantly higher materials loading and superior capacitive behavior compared to thin film electrodes formed on stainless steel current collectors. The electrodes obtained by pulse impregnation show higher specific capacitance compared to the electrodes prepared by galvanostatic impregnation.

1. Introduction

The growing interest in application of polypyrrole (PPY) for electrodes of electrochemical supercapacitors (ES) is attributed to high specific capacitance (SC), relatively large voltage window, high electrical conductivity, low cost, advanced chemical and mechanical properties of this material [1]. The high SC of PPY results from redox reactions, which allow charge storage in the bulk of the electrode material. Many fundamental investigations have been conducted with the objective to investigate the charging mechanism of PPY in different electrolytes and to utilize high theoretical SC of PPY (620 F g^{-1}) [1–4] in electrodes of ES.

The fabrication of PPY films by electropolymerization is an attractive technique that allows the pyrrole monomer, dissolved in a solvent, containing an anionic dopant, to be oxidized at the electrode surface by the applied anodic potential, forming a polymer film [5–7]. The anionic dopant is incorporated into the polymer to ensure electrical neutrality of the resulting film. Many studies were focused on modification of PPY based materials, optimization of film deposition conditions, and development of advanced anionic dopants [8–10]. Relatively high electrical conductivity and thermal stability of PPY films was achieved using aromatic anionic dopants [11–13]. It was shown that with the variation of the dopant anion, the conductivity of the PPY thin films can differ by three orders of magnitude [14]. The relatively high electrical conductivity and advanced electrochemical properties, achieved using *p*-toluenesulfonate, anthraquinone-2-sulfonate, benzenesulfonate and other dopants, resulted in intensive research

* Corresponding author. Tel.: +1 905 525 9140x23914; fax: +1 905 528 9295.
E-mail address: zhitom@mcmaster.ca (I. Zhitomirsky).

0378-7753/$ – see front matter © 2012 Elsevier B.V. All rights reserved.
http://dx.doi.org/10.1016/j.jpowsour.2012.08.017

on chemical interactions of PPY and aromatic anionic molecules [14–16]. Especially interesting are the investigations of composite materials containing carbon nanotubes in the PPY matrix [17,18]. Such composites showed reduced resistance and improved capacitive behavior. Also of great interest are the studies focused on the fabrication of PPY-metal oxide [19] and PPY-graphene [20–22] nanocomposites.

Despite the impressive progress achieved in the fabrication of PPY and composite electrodes of ES by electropolymerization, there is a need for further development of this method. One of the major challenges of electrochemical polymerization of pyrrole involves formation of adherent PPY films on non-noble metal substrates, as oxidation and dissolution of the substrates during anodic electropolymerization occurs readily. PPY based ES showed excellent capacitive behavior in H_2SO_4 [5,23] and HCl [8] electrolytes. The problems of corrosion of current collectors and chemical degradation of CNT in the acidic electrolytes can be diminished using Na_2SO_4 electrolyte [24]. However, the SC of PPY in Na_2SO_4 is usually lower, compared to that in acidic electrolytes.

PPY films were formed on low carbon steels using oxalic acid solution electrolyte [25]. It was shown that steels interacted with oxalic acid to form passive layers, which prevented corrosion of the substrates. However, the formation of the non-conductive and non-capacitive iron oxalate layer [26,27] results in increasing charge transfer resistance and reduced electrochemical capacitance of the PPY coated current collectors.

Recent studies [28] highlighted the importance of high active material loadings for the fabrication of efficient ES. However, the increase in material loading usually results in increased resistance and reduced SC. This problem can be addressed by the use of special current collectors, such as Ni foams or plaques. Previous investigations showed that Ni plaques [29], designed for high power applications, allowed significantly higher SC of MnO_2 electrodes, compared to MnO_2 electrodes based on Ni foams [30]. The advantages of Ni plaque based electrodes were especially evident at high charge–discharge rates. The important challenge is the electropolymerization of PPY on high surface area Ni plaque electrodes. Another strategy is based on the fabrication of PPY–CNT composites [17]. CNT are usually added to active materials in order to increase the electronic conductivity of the composite electrodes and improve the power density of ES. The use of CNT as conductive additives offers benefits of their high surface area and low percolation threshold. However, the specific capacitance of CNT is low. Therefore, the fabrication of PPY–CNT electrodes requires efficient dispersion of CNT in the PPY matrix and optimization of the CNT content in the composites. In order to achieve this goal, CNT must be well dispersed and negatively charged in the pyrrole solutions and incorporated into the growing PPY films. However, for CNT applications, which depend on electrical conductivity, it is challenging to achieve good dispersion, charging and controlled electrodeposition of pristine CNT and avoid defects due to chemical treatment or functionalization [17].

The goal of this investigation was the electrochemical fabrication of composite PPY–multiwalled carbon nanotubes (MWCNT) electrodes using stainless steel and Ni plaque current collectors. The approach is based on the use of organic dyes as anionic dopants for PPY electropolymerization. The comparison of the chemical structures and experimental data for pyrocatechol violet (PV) and *m*-cresol purple (CP) provided an insight into the deposition mechanism, which allowed the formation of adherent films using PV. The important finding was the possibility of efficient dispersion and controlled electrodeposition of MWCNT using PV as a dispersing agent. The results presented below showed that pulse deposition offers advantage of higher SC of Ni plaque based PPY–MWCNT composites, compared to the SC of similar electrodes prepared by the galvanostatic deposition.

2. Experimental procedures

Pyrrole, PV, CP (Aldrich), MWCNT (Arkema) were used for the fabrication of solutions and suspensions for electrodeposition. Commercial Ni plaques [31] were supplied by Vale Canada. Aqueous solutions of pyrrole, containing PV or CP were used for electropolymerization. PPY films were obtained galvanostatically at a current density of 1 mA cm^{-2} from 6.7 g L^{-1} pyrrole solutions, containing 1 g L^{-1} PV or CP. Potentiodynamic deposition of PPY films was performed at a scan rate of 20 mV s^{-1}. Electrophoretic deposition (EPD) of MWCNT was performed from aqueous suspensions, containing 0.1–1 g L^{-1} MWCNT and 0–1 g L^{-1} PV. The suspensions containing MWCNT were ultrasonicated for 30 min to achieve a homogeneous dispersion. Constant voltage EPD was performed at a deposition voltage of 20 V. Constant current EPD was performed at a current density of 1 mA cm^{-2}. Composite PPY–MWCNT deposits were obtained from aqueous 6.7 g L^{-1} pyrrole solutions, containing 0.1 g L^{-1} MWCNT and 1 g L^{-1} PV, using galvanostatic deposition or pulse deposition with ON and OFF times of 0.5 s at a current density of 1 mA cm^{-2}.

The electrodeposition cell included a substrate and Pt counter electrode. Stainless steel (grade 301) foil or Ni plaque substrates were used for deposition. The distance between the substrate and counter electrode was 15 mm. Deposition yield was studied at various PV concentrations and different deposition durations. A minimum of 3 samples were prepared in each deposition experiment. All the deposits were obtained using fresh solutions. The deposition yield measurements were repeatable and the error was less than 5%. Film adhesion was tested according to the ASTM D3359 standard.

The microstructure of the films was investigated using a JEOL JSM-7000F scanning electron microscope (SEM). Electrochemical studies were performed using a potentiostat (PARSTAT 2273, Princeton Applied Research). Surface area of the working electrode was 1 cm^2. The counter electrode was a platinum gauze, and the reference electrode was a standard calomel electrode (SCE). Capacitive behavior and electrochemical impedance of the films were investigated in 0.5 M Na_2SO_4 aqueous solutions. Cyclic voltammetry (CV) studies were performed within a potential range of −0.5 to +0.4 V versus SCE at scan rates of 2–100 mV s^{-1}. The specific capacitance (SC) was calculated using half the integrated area of the CV curve to obtain the charge (Q), and subsequently dividing the charge by the film mass (m) and width of the potential window (ΔV):

$$C = \frac{Q}{m\Delta V} \quad (1)$$

Impedance spectroscopy investigations were performed in the frequency range of 0.1 Hz–100 kHz, the amplitude of the applied voltage was 5 mV.

3. Results and discussion

Fig. 1 shows chemical structures of PV and CP molecules used in this investigation. PV and CP are polyaromatic compounds with similar structures. The anionic properties of the molecules are related to their SO_3^- groups. The structure of PV includes two OH groups bonded to the adjacent carbon atoms of the aromatic ring. PV and CP were investigated as anionic dopants for electropolymerization of PPY and as charging and dispersing agents for the electrodeposition of MWCNT.

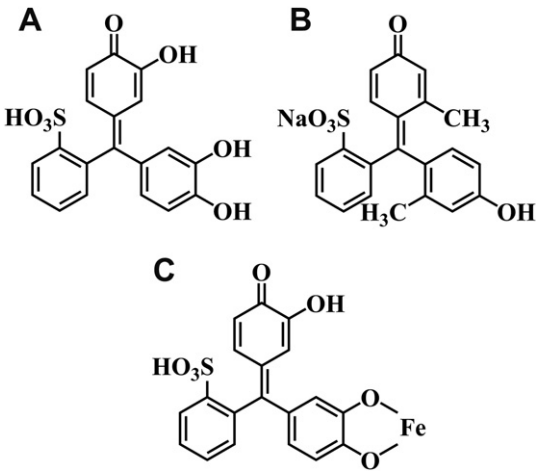

Fig. 1. Chemical structures of (A) PV, (B) CP and (C) PV–Fe complex.

Electropolymerization of PPY was performed at potentiodynamic and galvanostatic conditions. The potentiodynamic curves recorded for stainless steel electrode in pyrrole solutions, containing PV, were presented in Fig. 2A. The CV data for the first scan showed that the increase in electrode potential above ~0.6 V resulted in increasing current, attributed to electropolymerization of PPY. Indeed, black films were formed at the stainless steel electrode at higher potentials. In the subsequent scans, a slight progressive increase of current was observed, indicating the continuous growth of conductive film without passivation or corrosion [32–35]. Such behavior also indicates that the electronic conductivity of the film is sufficiently high to consider the ohmic potential drop inside the film as negligible [36,37]. In contrast, the formation of a passivation layer usually results in the reduction of current with increasing cycle number [38].

PPY films were also formed under galvanostatic mode using PV additive. The potential versus time dependence at a current density of 1 mA cm^{-2} (Fig. 2B) indicated that there is no induction time for electropolymerization of PPY. At the beginning of the electrodeposition process, the potential difference between the working and reference electrode increased and then slightly decreased to a steady value (Fig. 2B). In contrast, literature data [26,39] on deposition from pyrrole solutions, containing oxalic acid, revealed the presence of an induction period, related to the dissolution of iron and formation of an iron oxalate layer. The deposit mass versus time dependence presented in Fig. 2C was nearly linear and indicated continuous film growth without induction time. The measurements of film adhesion according to the ASTM D3359 standard showed that adhesion strength corresponded to the 4B classification. When CP was used as an anionic dopant for PPY electropolymerization, patchy deposition was observed. The deposits, prepared using CP, showed poor adhesion.

The comparison of the chemical structures of PV and CP (Fig. 1A, B) indicated that OH groups of PV, bonded to adjacent carbon atoms of the aromatic ring, exert influence on the formation of PV doped PPY films on stainless steel substrates. Such groups can provide catecholate type of bonding with metal atoms on the substrate surface and improve film adhesion. The interest in application of molecules from the catechol family for the development of adherent coatings has resulted from the fundamental investigations of biomimetic adhesion [40,41], which was attributed to the chelation of catecholic amino acid, L-3,4-dihydroxyphenylalanine (DOPA). The remarkable adhesion strength provided by DOPA containing proteins to inorganic surfaces in marine environment has generated significant research activity focused on the development of advanced adhesives with improved stability in aqueous solutions of inorganic salts and novel dispersing agents with strong interfacial adhesion [42–44]. It has been demonstrated that materials from catechol and gallate families, containing OH groups bonded to the adjacent carbon atoms of the aromatic ring, strongly adsorbed on various inorganic materials [42,43,45]. It is important to note that such bonds improved charge transfer between inorganic and organic materials [45]. Fig. 3C shows the catecholate type bonding mechanism of PV [44], involving the deprotonation of OH groups and complexation of Fe atoms on the substrate surface.

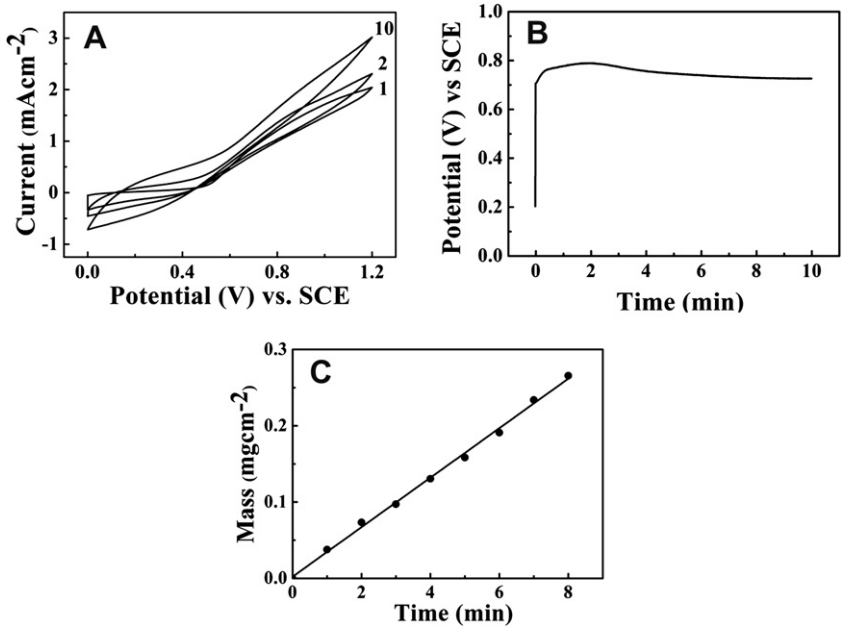

Fig. 2. Electrodeposition of PPY from 6.7 g L^{-1} pyrrole solution, containing 1 g L^{-1} PV: (A) cyclic voltammetry data at a scan rate of 20 mV s^{-1}, the cycle numbers are indicated, (B) potential and (C) deposit mass versus time dependencies at a current density of 1 mA cm^2.

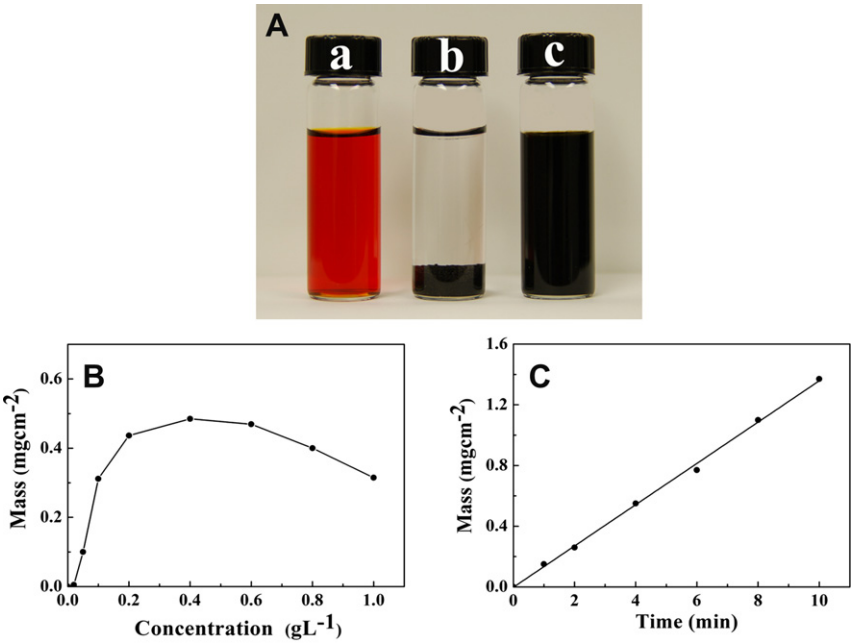

Fig. 3. (A) (a) Aqueous solution of PV, (b) MWCNT in water, (c) MWCNT in aqueous PV solution, (B) deposit mass versus PV concentration in 1 g L^{-1} MWCNT suspension at a deposition voltage of 20 V and deposition time of 6 min, (C) deposit mass versus deposition time for 1 g L^{-1} MWCNT suspension, containing 1 g L^{-1} PV at a current density of 1 mA cm^{-2}.

The results described so far showed the possibility of the formation of adherent PPY films on stainless steel substrates. In addition, adherent PPY films were obtained on Ni substrates using PV as a dopant. Moreover, the use of PV allowed the formation of composite PPY–MWCNT films. It was found that PV allowed the formation of stable suspensions of negatively charged MWCNT, controlled EPD of MWCNT and electrochemical co-deposition of PPY and MWCNT.

Sedimentation experiments revealed excellent colloidal stability of MWCNT suspensions, containing PV. The suspensions with PV/MWCNT mass ratio of 0.2–1.0 were stable for more than 3 months (Fig. 3A). The addition of PV to the MWCNT suspensions allowed the formation of MWCNT films by anodic EPD. The MWCNT films were obtained by constant voltage and constant current deposition methods. It is suggested that PV adsorbed on the surface of MWCNT and provided electrosteric stabilization. Moreover, the adsorbed PV provided a negative charge required for anodic deposition of MWCNT. The mechanism of PV adsorption on MWCNT was related to π–π interactions.

Fig. 3B shows the influence of PV concentration on the deposition yield. It should be noted that the influence of additive concentration on the EPD deposition yield is usually studied at constant voltage conditions [46], because additives can change the suspension conductivity. It is in this regard that EPD involves the motion of charged particles under the influence of an electric field. When EPD is performed in the constant voltage mode, the electric field is the same for suspensions with different additive concentrations [46]. The deposition yield increased with increasing PV concentration (Fig. 3B), showed a maximum and then decreased at PV concentrations above 0.6 g L^{-1}. It should be noted that EPD method is based on the use of stable suspensions of charged particles. Electrophoretic motion results in accumulation of the particles at the electrode surface. Deposit formation is achieved via particle coagulation. Previous investigations showed that mutual electrostatic repulsions of the charged particles at the electrode surface can reduce the deposition yield or prevent deposit formation [47]. It is suggested that the increase in PV concentration in the suspensions resulted in increased charge of MWCNT, which resulted in enhanced mutual electrostatic repulsions of MWCNT at the electrode surface and reduced deposition yield (Fig. 3B). The deposit mass increased with increasing deposition time. Nearly linear dependence was obtained using a constant current deposition method (Fig. 3C). The results indicated the possibility of controlled deposition of films of different mass and showed relatively high deposition rate.

The use of PV offers important advantages for the MWCNT dispersion and electrodeposition, such as high suspension stability and high deposition rate. In the previous investigations, various methods were developed for the dispersion and EPD of CNT. It was found that adsorbed anionic and cationic polyelectrolytes provided charging of CNT in suspensions and allowed the formation of anodic or cathodic deposits by EPD [48]. Significant effort has been invested in the development of functionalization strategies, which included both covalent and supramolecular approaches [49–51]. However, polymer “wrapping” and supramolecular dispersion methods often result in the formation of CNT bundles.

The interactions of CNT with charging additives and solvents are especially important for EPD technology [52]. Many attempts have been made to improve wetting properties of carbon nanotubes in solvents by oxidation in strong acids or mixtures of acids [52,53]. It was shown that under acidic conditions, defective sites in the CNT are attacked, resulting in the formation of fragmented CNT, decorated with carboxylic and other oxygen-containing groups on their surface. These acidic groups electrostatically stabilized the CNT in suspensions and provided a negative charge for EPD. However, the oxidation and functionalization strategies introduce defects on the CNT sidewalls and reduce electronic conductivity of CNT. In another approach, the charging of CNT for EPD was achieved by adsorption of metal ions from added metal salts [52,54]. It should be noted that the addition of metal salts results in lower suspension stability, attributed to increasing ionic strength of the suspension. The metal ions usually incorporate into the deposits as corresponding hydroxides or oxides and contaminate the deposits.

The dispersion and EPD of CNT using surfactants is of special interest [51]. Sodium dodecyl sulfate (SDS) is one of the most promising anionic surfactants for the fabrication of stable suspensions of CNT [51]. However, relatively large concentration of SDS is required for CNT dispersion and EPD [55]. SDS form micelles, which induce a depletion attraction between the nanotubes [56,57]. The strength of the attraction increases with increasing micelle concentration. As a result the increase in SDS concentration results in CNT aggregation. Van der Waals − induced aggregation at low SDS concentration and depletion-induced aggregation at high SDS concentration define an intermediate concentration range, where CNT can be homogeneously dispersed. The width of this SDS concentration range decreases drastically with increasing CNT concentration [56,57], preventing the dispersion. It should be noted that the mechanism of PV adsorption on MWCNT is different from the mechanism of SDS adsorption. It is suggested that π–π interactions allow strong adsorption of PV on MWCNT, improved dispersion and EPD of MWCNT films.

The results presented above (Fig. 2C and Fig. 3C) indicated that PPY and MWCNT can be deposited at similar conditions on stainless steel substrates using PV additive. The use of PV allowed controlled deposition of both materials. These results pave the way for the deposition of composite PPY–MWCNT films from pyrrole solutions containing PV and MWCNT, using PV as an anionic dopant for PPY and dispersing agent for MWCNT. The method for the fabrication of PPY–MWCNT composite films involved electropolymerization of PPY and EPD of MWCNT. Fig. 4 shows SEM images of PPY, MWCNT and composite PPY–MWCNT films and corresponding pictures of the deposits on stainless steel substrates. The films were continuous and crack free. The SEM image of PPY film (Fig. 4A) showed that the film contained nanoparticles with size below 100 nm. The film porosity can be attributed to gas evolution during electropolymerization. Fig. 4B shows the surface morphology of the MWCNT films. The film contained non-agglomerated MWCNT, which formed a continuous network. Fig. 4C shows nanoparticles of PPY and MWCNT and confirms the formation of composite films. The MWCNT were well dispersed and formed a conductive network. The PPY nanoparticles were deposited between MWCNT. Moreover, the SEM image showed that some MWCNT were coated with PPY. The film showed enhanced porosity, compared to pure PPY and MWCNT films. The microstructure of the composite film (Fig. 4C) is beneficial for electrodes of ES, because dispersed MWCNT can provide improved electronic conductivity, whereas film porosity allows electrolyte access to the active material.

The films deposited on stainless steel substrates showed capacitive behavior in 0.5 M Na_2SO_4 electrolyte. Fig. 5A shows SC versus scan rate dependence and corresponding CV at 20 mV s^{-1} for 160 μg cm^{-2} PPY–MWCNT film. The SC of 224 F g^{-1} was obtained at a scan rate of 2 mV s^{-1}. The SC decreased significantly with increasing scan rate due to diffusion limitation in pores. The SC at the scan rate of 100 mV s^{-1} was found to be 73 F g^{-1}. Fig. 5B shows Nyquist plot for complex impedance $Z^* = Z' - iZ''$. The impedance data for conductive polymer films are usually analyzed using an equivalent circuit [58,59] including solution resistance, charge transfer resistance and capacitances or constant phase elements.

The depressed semicircle at high frequencies indicated the contribution of charge transfer resistance [59] at the interface between the electrolyte and PPY electrode. Similar to other investigations [59], the low frequency slope deviated from 90° and indicated the contribution of Warburg diffusion. The increase in film mass resulted in reduced SC and increasing impedance. However, the material loading can be increased using Ni plaques as current collectors and higher SC can be achieved. Fig. 6A shows SC versus scan rate and corresponding CVs for composite PPY–MWCNT materials with mass of 350 and 660 μg cm^{-2}, electrochemically impregnated into Ni plaques. The electrode with material loading of 350 μg cm^{-2}, showed a SC of 375 F g^{-1} at a scan rate of 2 mV s^{-1}. The difference between the electrode formed on stainless steel and Ni plaque current collectors is especially evident at high scan rates. At a scan rate of 100 mV s^{-1} the Ni plaque based electrode with material loading of 350 μg cm^{-2} showed 3 times

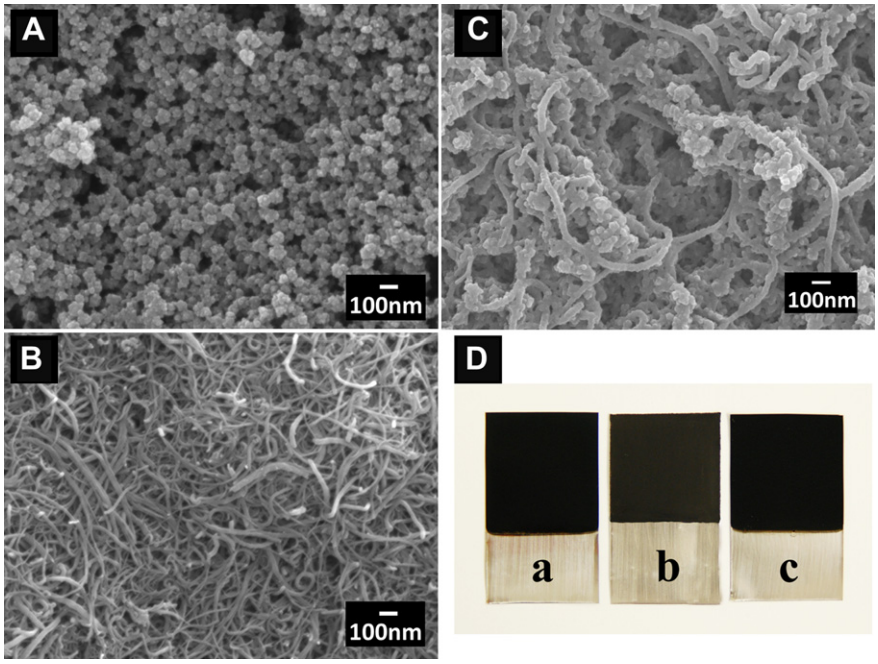

Fig. 4. SEM images of films prepared at a current density of 1 mA cm^{-2}: (A) PPY, deposited from 6.7 g L^{-1} pyrrole solution, containing 1 g L^{-1} PV (B) MWCNT, deposited from 1 g L^{-1} MWCNT suspension, containing 1 g L^{-1} PV (C) composite PPY–MWCNT, deposited from 6.7 g L^{-1} pyrrole solution, containing 1 g L^{-1} PV and 0.1 g L^{-1} MWCNT, and corresponding pictures of the films on stainless steel substrates (D) (a) PPY, (b) MWCNT and (c) PPY–MWCNT.

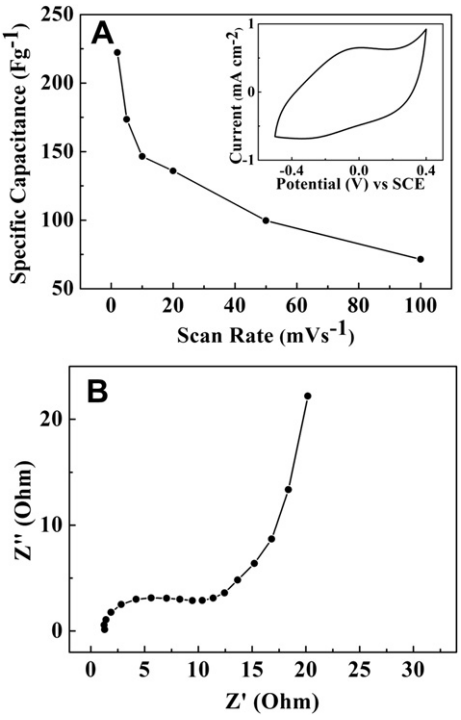

Fig. 5. (A) SC versus scan rate, inset shows CV at a scan rate of 20 mV s^{-1} and (B) Nyquist plot for complex impedance $Z^* = Z' - iZ''$ for composite 160 μg cm^{-2} PPY–MWCNT film deposited on stainless steel substrate from 6.7 g L^{-1} pyrrole solution, containing 1 g L^{-1} PV and 0.1 g L^{-1} MWCNT at a current density of 1 mA cm^{-2}.

larger SC compared to the thin film electrode on a stainless substrate with film mass of 160 μg cm^{-2}. The electrochemical impedance studies (Fig. 6B(a)) showed significantly lower impedance of the Ni plaque based electrode. The high frequency semicircle practically disappeared, indicating reduced charge transfer resistance. However, the increase in material loading resulted in reduced SC and increased impedance (Fig. 6). Further improvement was achieved using a pulse deposition method. Fig. 7 compares capacitive behavior and impedance data for the 1 mg cm^{-2} films prepared by galvanostatic and pulse deposition methods. The film deposited by the pulse method showed SC of 390 and 210 F g^{-1} at scan rates of 2 and 100 mV s^{-1}, respectively. The film prepared by galvanostatic deposition exhibited much lower capacitance. The comparison of the corresponding impedance data indicated reduced impedance of the electrode prepared by the pulse deposition method. The analysis of available literature [10,60] indicated that the PPY films prepared by pulse deposition exhibited much higher SC compared to the films prepared galvanostatically. The improved capacitive behavior is usually attributed to higher porosity and lower particle size of the films prepared by pulse deposition method. The higher porosity and lower particle size allow better electrolyte access to active material.

The microstructures of the PPY–MWCNT electrodes, prepared by impregnation of Ni plaques, were studied by SEM. Commercial Ni plaques used in this study consisted of a perforated Ni foil and sintered filamentary Ni particles, which formed a porous network. Fig. 8(A, B) shows SEM images of the surface of a Ni plaque at different magnifications. The plaques exhibited porous microstructure with pore sizes in the range of 0–20 μm (Fig. 8(A)). The SEM image obtained at higher magnification (Fig. 8(B)) showed that the size of Ni particles was in the range of 0.5–2 μm. The porosity and conductivity of commercial Ni plaques are beneficial for their application as current collectors of ES. SEM studies showed that

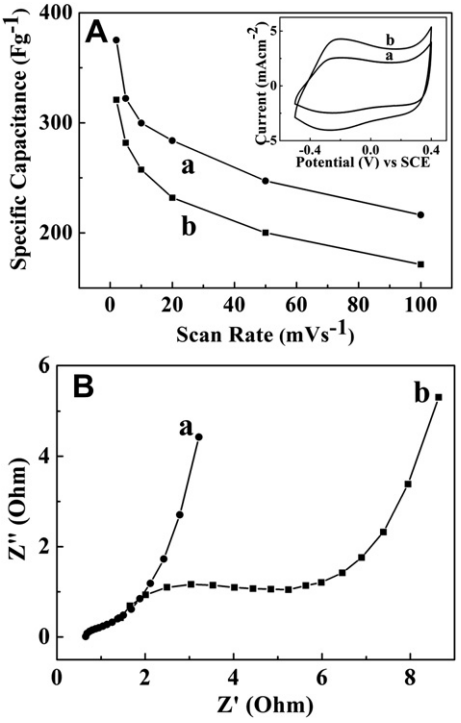

Fig. 6. (A) SC versus scan rate, inset shows corresponding CVs at a scan rate of 20 mV s^{-1} and (B) Nyquist plots for complex impedance $Z^* = Z' - iZ''$ for composite PPY–MWCNT material with mass of (a) 350 and (b) 660 μg cm^{-2}, electrochemically impregnated into Ni plaques from 6.7 g L^{-1} pyrrole solution, containing 1 g L^{-1} PV and 0.1 g L^{-1} MWCNT at a current density of 1 mA cm^{-2}.

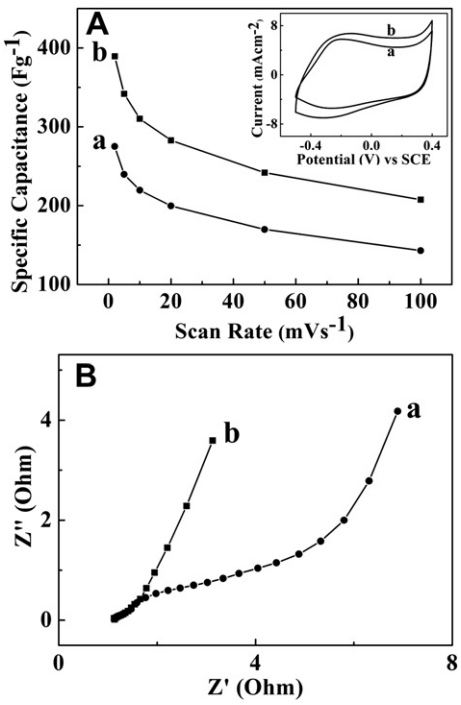

Fig. 7. (A) SC versus scan rate, inset shows corresponding CVs at a scan rate of 20 mV s^{-1} and (B) Nyquist plots for complex impedance $Z^* = Z' - iZ''$ for composite PPY–MWCNT material with mass of 1 mg cm^{-2}, electrochemically impregnated into Ni plaques from 6.7 g L^{-1} pyrrole solution, containing 1 g L^{-1} PV and 0.1 g L^{-1} MWCNT at a current density of 1 mA cm^{-2} by (a) galvanostatic and (b) pulse deposition methods.

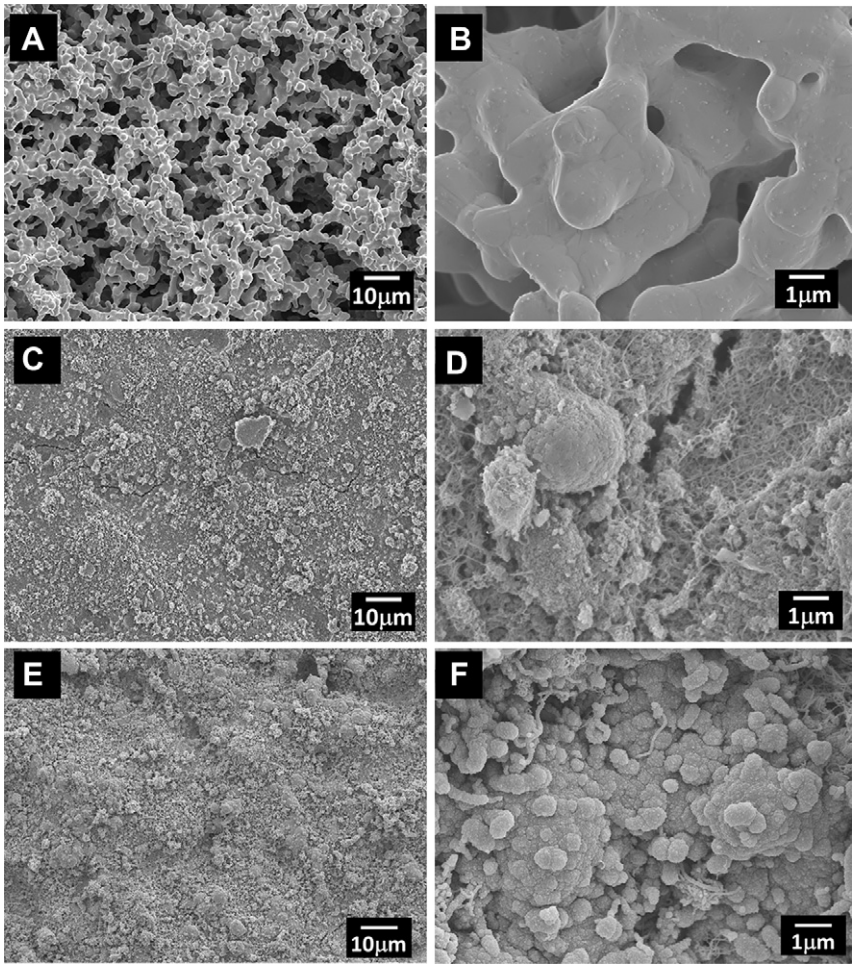

Fig. 8. SEM images at different magnifications of (A, B) as-received plaques, (C–F) electrochemically impregnated plaques with 1 mg cm^{-2} PPY–MWCNT from 6.7 g L^{-1} pyrrole solution, containing 1 g L^{-1} PV and 0.1 g L^{-1} MWCNT at a current density of 1 mA cm^{-2} by (C, D) galvanostatic and (E, F) pulse deposition methods.

plaques were impregnated with composite PPY–MWCNT material. However, in the galvanostatic deposition method, the increase in material loading resulted in accumulation of the material on the surface of the Ni plaques. The SEM studies of the impregnated plaques at material loading of 1 mg cm^{-2} revealed cracks (Fig. 8(C, D)). It is suggested that some large unfilled pores below the material, deposited at the plaque surface, promoted crack formation. In contrast, cracks in the deposits were avoided using the pulse method (Fig. 8(E, F)). The pulse method allowed improved impregnation of the Ni plaques. The SEM images revealed relatively rough morphology due to the surface roughness of the Ni plaques. Some large pores remained open at material loading of 1 mg cm^{-2}. The comparison of the SEM images for the plaques impregnated by galvanostatic and pulse methods revealed relatively large number of MWCNT accumulated at the surface of the galvanostatically impregnated plaques. It is suggested that impregnation was hindered by the MWCNT, accumulated at the plaque surface in the galvanostatic method. The improved impregnation of the Ni plaques in the pulse method and remaining open porosity of the electrode resulted in better electrochemical performance. It is in this regard that pulse impregnation method [29] allowed more efficient impregnation of Ni plaques with MnO_2 and provided higher SC, compared to the galvanostatic impregnation method. The PPY–MWCNT loading achieved in this investigation was comparable with loading of MnO_2 reported in the previous investigation [29]. Recent studies highlighted the importance of volume loading of porous current collectors with active material [28]. It is in this regard that PPY and MWCNT have significantly lower density, compared to the density of MnO_2.

It should be noted that Ni plaques are widely used in battery technology. Electrodes are formed by electrosynthesis of $Ni(OH)_2$ in pores of Ni plaque current collectors [31]. Previous studies showed that electrosynthesis of MnO_2 can be used for the impregnation of Ni plaques and the fabrication of electrodes of ES. The results presented above indicated that Ni plaques, electrochemically impregnated with PPY–MWCNT, are promising electrodes for ES. However, further investigations are necessary for the optimization of the impregnation method, composition and properties of the electrodes.

4. Conclusions

Adherent PPY films were obtained on stainless steel and Ni substrates by electropolymerization, using PV additive from the catechol family as an anionic dopant. The comparison of the experimental data for PV, containing OH groups bonded to adjacent carbon atoms of the aromatic ring, and CP without such groups, showed that the interaction OH groups with metal atoms at the substrate surface promoted film adhesion. It was found that PV allows efficient dispersion, charging and controlled EPD of MWCNT films. Composite PPY–MWCNT films were obtained by a combined electrodeposition method using PV as an anionic dopant for PPY

electropolymerization and as a charged dispersant for EPD of MWCNT. The composite materials deposited as thin films on stainless steel foils or impregnated into Ni-plaque current collectors showed capacitive behavior in 0.5 M Na_2SO_4 electrolyte.

Ni plaque based electrodes offer advantages of significantly higher materials loading and superior capacitive behavior compared to thin film electrodes formed on stainless steel current collectors. The electrodes obtained by pulse impregnation showed higher specific capacitance compared to the electrodes prepared by galvanostatic impregnation. The highest SC of 390 F g^{-1} was achieved at a scan rate of 2 mV s^{-1} for 1 mg cm^{-2} electrodes, prepared by pulse impregnation of Ni plaques.

Acknowledgments

The authors gratefully acknowledge the financial support of the Natural Sciences and Engineering Research Council of Canada.

References

[1] G.A. Snook, P. Kao, A.S. Best, Journal of Power Sources 196 (2011) 1–12.
[2] X. Lu, H. Dou, C. Yuan, S. Yang, L. Hao, F. Zhang, L. Shen, L. Zhang, X. Zhang, Journal of Power Sources 197 (2012) 319–324.
[3] B.C. Kim, C.O. Too, J.S. Kwon, J.M. Ko, G.G. Wallace, Synthetic Metals 161 (2011) 1130–1132.
[4] H. An, Y. Wang, X. Wang, L. Zheng, X. Wang, L. Yi, L. Bai, X. Zhang, Journal of Power Sources 195 (2010) 6964–6969.
[5] D.P. Dubal, S.H. Lee, J.G. Kim, W.B. Kim, C.D. Lokhande, Journal of Materials Chemistry 22 (2012) 3044–3052.
[6] A. Faye, G. Dione, M.M. Dieng, J.J. Aaron, H. Cachet, C. Cachet, Journal of Applied Electrochemistry 40 (2010) 1925–1931.
[7] B. Muthulakshmi, D. Kalpana, S. Pitchumani, N.G. Renganathan, Journal of Power Sources 158 (2006) 1533–1537.
[8] J. Wang, Y. Xu, J. Wang, X. Du, Synthetic Metals 161 (2011) 1141–1144.
[9] R. Ramya, M.V. Sangaranarayanan, Journal of Chemical Sciences 120 (2008) 25–31.
[10] R.K. Sharma, A.C. Rastogi, S.B. Desu, Electrochemistry Communications 10 (2008) 268–272.
[11] I. Carrillo, E.S. De La Blanca, M.I. Redondo, M.V. Garcia, M.J. Gonzalez-Tejera, J.L.G. Fierro, E. Enciso, Synthetic Metals 162 (2012) 136–142.
[12] G.R. Mitchell, F.J. Davis, C.H. Legge, Synthetic Metals 26 (1988) 247–257.
[13] D. Lesueur, N.D. Alberola, Synthetic Metals 88 (1997) 133–138.
[14] P.-C. Wang, J.-Y. Yu, Reactive and Functional Polymers 72 (2012) 311–316.
[15] J. Tamm, T. Raudsepp, M. Marandi, T. Tamm, Synthetic Metals 157 (2007) 66–73.
[16] T. Raudsepp, M. Marandi, T. Tamm, V. Sammelselg, J. Tamm, Electrochimica Acta 53 (2008) 3828–3835.
[17] J. Wang, Y. Xu, F. Yan, J. Zhu, J. Wang, F. Xiao, Journal of Solid State Electrochemistry 14 (2010) 1565–1575.
[18] J. Wang, Y. Xu, X. Chen, X. Sun, Composites Science and Technology 67 (2007) 2981–2985.
[19] R.K. Sharma, A. Karakoti, S. Seal, L. Zhai, Journal of Power Sources 195 (2010) 1256–1262.
[20] H.-H. Chang, C.-K. Chang, Y.-C. Tsai, C.-S. Liao, Carbon 50 (2012) 2331–2336.
[21] J. Wang, Y. Xu, J. Zhu, P. Ren, Journal of Power Sources 208 (2012) 138–143.
[22] D. Zhang, X. Zhang, Y. Chen, P. Yu, C. Wang, Y. Ma, Journal of Power Sources 196 (2012) 5990–5996.
[23] D.P. Dubal, S.V. Patil, W.B. Kim, C.D. Lokhande, Materials Letters 65 (2011) 2628–2631.
[24] S.R. Sivakkumar, J.M. Ko, D.Y. Kim, B.C. Kim, G.G. Wallace, Electrochimica Acta 52 (2007) 7377–7385.
[25] W. Su, J.O. Iroh, Journal of Applied Polymer Science 65 (1997) 417–424.
[26] W.J. Hamer, L. Koene, J.H.W. De Wit, Materials and Corrosion 55 (2004) 653–658.
[27] K.H. An, K.K. Jeon, J.K. Heo, S.C. Lim, D.J. Bae, Y.H. Lee, Journal of the Electrochemical Society 149 (2002) A1058–A1068.
[28] Y. Gogotsi, P. Simon, Science 334 (2011) 917–918.
[29] Y. Wang, Q. Min Yang, I. Zhitomirsky, Materials and Manufacturing Processes 26 (2011) 846–854.
[30] J. Li, Q.M. Yang, I. Zhitomirsky, Journal of Power Sources 185 (2008) 1569–1574.
[31] A.Y. Zaitsev, D.S. Wilkinson, G.C. Weatherly, T.F. Stephenson, Journal of Power Sources 123 (2003) 253–260.
[32] L.M. Martins Dos Santos, J.C. Lacroix, K.I. Chane-Ching, A. Adenier, L.M. Abrantes, P.C. Lacaze, Journal of Electroanalytical Chemistry 587 (2006) 67–78.
[33] M.B. Gonzalez, S.B. Saidman, Corrosion Science 53 (2011) 276–282.
[34] V. Annibaldi, A.D. Rooney, C.B. Breslin, Corrosion Science 59 (2012) 179–185.
[35] M. Bazzaoui, J.I. Martins, T.C. Reis, E.A. Bazzaoui, M.C. Nunes, L. Martins, Thin Solid Films 485 (2005) 155–159.
[36] J.P. Correia, M. Graczyk, L.M. Abrantes, M.A. Vorotyntsev, Electrochimica Acta 53 (2007) 1195–1206.
[37] P.A. Mabrouk, Synthetic Metals 150 (2005) 101–105.
[38] M.I. Redondo, C.B. Breslin, Corrosion Science 49 (2007) 1765–1776.
[39] A. De Bruyne, J.L. Delplancke, R. Winand, Surface and Coatings Technology 99 (1998) 118–124.
[40] J.H. Waite, Nature Materials 7 (2008) 8–9.
[41] L. Haeshin, S.M. Dellatore, W.M. Miller, P.B. Messersmith, Science 318 (2007) 426–430.
[42] Y. Wang, I. Zhitomirsky, Langmuir 25 (2009) 9684–9689.
[43] K. Wu, Y. Wang, I. Zhitomirsky, Journal of Colloid and Interface Science 352 (2010) 371–378.
[44] Y. Sun, M.S. Ata, I. Zhitomirsky, Journal of Colloid and Interface Science 369 (2012) 395–401.
[45] G.-L. Wang, J.-J. Xu, H.-Y. Chen, Biosensors and Bioelectronics 24 (2009) 2494–2498.
[46] I. Zhitomirsky, A. Petric, Journal of Materials Science 39 (2004) 825–831.
[47] I. Zhitomirsky, Advances in Colloid and Interface Science 97 (2002) 277–315.
[48] K. Grandfield, F. Sun, M. FitzPatrick, M. Cheong, I. Zhitomirsky, Surface and Coatings Technology 203 (2009) 1481–1487.
[49] T. Casagrande, G. Lawson, H. Li, J. Wei, A. Adronov, I. Zhitomirsky, Materials Chemistry and Physics 111 (2008) 42–49.
[50] K. Wu, P. Imin, Y. Sun, X. Pang, A. Adronov, I. Zhitomirsky, Materials Letters 67 (2012) 248–251.
[51] L. Vaisman, H.D. Wagner, G. Marom, Advances in Colloid and Interface Science 128-130 (2006) 37–46.
[52] A.R. Boccaccini, J. Cho, J.A. Roether, B.J.C. Thomas, E. Jane Minay, M.S.P. Shaffer, Carbon 44 (2006) 3149–3160.
[53] K. Esumi, M. Ishigami, A. Nakajima, K. Sawada, H. Honda, Carbon 34 (1996) 279–281.
[54] C. Du, N. Pan, Nanotechnology 17 (2006) 5314–5318.
[55] S. Pei, J. Du, Y. Zeng, C. Liu, H.-M. Cheng, Nanotechnology 20 (2009) 235707.
[56] B. Vigolo, C. Coulon, M. Maugey, C. Zakri, P. Poulin, Science 309 (2005) 920–923.
[57] B. Vigolo, A. Penicaud, C. Coulon, C. Sauder, R. Pailler, C. Journet, P. Bernier, P. Poulin, Science 290 (2000) 1331–1334.
[58] S. Biswas, L.T. Drzal, Chemistry of Materials 22 (2010) 5667–5671.
[59] W. Sun, R. Zheng, X. Chen, Journal of Power Sources 195 (2012) 7120–7125.
[60] J. Wang, Y. Xu, J. Wang, X. Du, F. Xiao, J. Li, Synthetic Metals 160 (2010) 1826–1831.